

## Research Article

# Calibration of Microscopic Traffic Flow Simulation Models considering Subsets of Links and Parameters

Alexander Paz <sup>1</sup>, Kul Shrestha <sup>2</sup>, Cristian Arteaga <sup>3</sup> and Douglas Baker <sup>4</sup>

<sup>1</sup>School of Civil Engineering, Queensland University of Technology, Brisbane 4001, Australia

<sup>2</sup>NOVA Geotechnical & Inspection Services, Las Vegas, NV 89118, USA

<sup>3</sup>Department of Civil and Environmental Engineering and Construction, University of Nevada, Las Vegas 89154, NV, USA

<sup>4</sup>School of Built Environment, Queensland University of Technology, Brisbane 4001, Australia

Correspondence should be addressed to Alexander Paz; [alexander.paz@qut.edu.au](mailto:alexander.paz@qut.edu.au)

Received 12 June 2020; Revised 10 October 2020; Accepted 19 October 2020; Published 31 October 2020

Academic Editor: Vittorio Astarita

Copyright © 2020 Alexander Paz et al. This is an open access article distributed under the Creative Commons Attribution License, which permits unrestricted use, distribution, and reproduction in any medium, provided the original work is properly cited.

This study proposes a methodology for the calibration of microscopic traffic flow simulation models by enabling simultaneous selection of traffic links and associated parameters. The analyst selects any number and combination of links and model parameters for calibration. Most calibration methods consider the entire network and use ad hoc approaches without enabling a specific selection of location and associated parameters. In practice, only a subset of links and parameters is used for calibration based on several factors such as expert knowledge of the system or constraints imposed by local governance. In this study, the calibration problem for the simultaneous selection of links and parameters was formulated using a mathematical programming approach. The proposed methodology is capable of calibrating model parameters considering multiple time periods and performance measures simultaneously. Traffic volume and speed are the performance measures used in this study, and the methodology is developed without considering the characteristics of a specific traffic flow model. A genetic algorithm was implemented to find a solution to the proposed mathematical program. In the experiments, two traffic models were calibrated: the first set of experiments included selection of links only, while all associated parameters were considered for calibration. The second set of experiments considered simultaneous selection of links and parameters. The implications of these experiments indicate that the models were calibrated successfully subject to selection of a minimum number of links. As expected, the more links and parameters that are used for calibration, the more time it takes to find a solution, but the overall results are better. All parameter values were reasonable and within constraints after successful calibration.

## 1. Introduction

Microscopic traffic flow simulation is increasingly being used to analyze complex scenarios for a broad range of objectives. One of the most important and challenging aspects for obtaining meaningful results is calibration, which involves adjusting the model parameters to enhance the ability of the model to generate local traffic conditions [1–3]. Existing calibration approaches propose various optimization algorithms and varying sets of calibration parameters. Sequential as well as simultaneous calibration of model parameters are proposed in the literature.

The calibration approach provided by the Federal Highway Administration (FHWA) in Traffic Analysis

Toolbox Volume IV suggests a sequential process of calibrating the capacity at key bottlenecks, traffic volumes, and system performance [2]. Using this approach, model parameters are adjusted by modifying global parameters first, then link parameters, and finally route choice parameters. Ma et al. [4] used a sequential approach to calibrate global and local parameters separately. Jha et al. [5] calibrated driver-behavior parameters separately from other parameters, such as route choice factors and origin-destination (O-D) flows. Paz et al. [3, 6] used an iterative approach where one group of parameters was calibrated, while others remained fixed. Issues associated with the use of a sequential calibration process include difficulty to achieve convergence and stable solutions [6].

Many mathematical programming formulations have been proposed to characterize and solve the problem of calibrating simulation-based traffic flow models. A simplex algorithm was proposed to calibrate microscopic traffic flow simulation models using intelligent transportation system data [7]. The proposed algorithm was very effective for congested conditions compared to simple manual calibration techniques. However, this effectiveness decreased as congestion decreased. The proposed approach considers only a single objective to minimize the difference between observed and estimated volume. In practice, multiple objectives are likely to be required.

Various genetic algorithms (GAs) have been proposed to calibrate microscopic simulation models [4, 5, 8–14] with successful results and relatively faster convergence. Yang et al. [15] proposed an orthogonal genetic algorithm (OGA) that provided superior results when compared to a GA; however, the number of calibrated parameters was few. In contrast, GA was found to converge relatively quickly for simulation models with many parameters [10]. Simultaneous perturbation stochastic approximation (SPSA) algorithms have also been widely used to calibrate microscopic simulation models [4, 16–19]. SPSA was found to provide a similar level of accuracy, fewer iterations, and less computation time than GAs and the trial-and-error iterative adjustment (IA) algorithms [16]. A memetic algorithm (MA) was found to be superior to a SPSA algorithm because the fine-tuning process required was significantly quicker for MA [3]. Cobos et al. [20] found that when a MA was adapted, using Solis and Wets local search chains (MA-SW-Chains), the results provided better and faster convergence compared to both SPSA and MA. A multiobjective MA based on NSGA-II and simulated annealing (NSGA-II-SA) also offered better results for runtime and convergence compared to a single-objective MA [21]. Considering that the performance of the calibration process and the time invested in finding the correct set of hyperparameters are correlated and affected by the characteristics of each metaheuristic, 17 alternative algorithms including multi- and mono-objective approaches were evaluated [22]. An adaptation of the global-best harmony search provided the best results considering both stability and dominance.

Microscopic traffic flow simulation models use the concept of car-following and lane-changing theories to represent vehicle interactions and driver-behavior dynamics [2, 23]. Typically, calibration parameters are related to driver characteristics, such as car-following behavior and gap acceptance. Balakrishna et al. [16] proposed the calibration of demand-and-supply parameters simultaneously. However, the calibration was performed only with link counts and used precalibrated values for the driver-behavior parameters. Cheu et al. [8] used parameters such as free-flow speeds, car-following distance, car-following sensitivity factors, lag-to-accelerate/decelerate factors, and lane-changing factors. Results showed that free-flow speeds, car-following distance, and car-following sensitivity factors had the most effect and are important for calibration; thus, calibration could be performed using only these three parameters. Ma and Kim [4, 13] considered calibration parameters that were

associated with acceleration/deceleration, car-following, and lane-changing behaviors. The lane-change probability and car-following distance were found to have relatively close calibrated and default values, suggesting that calibration could be performed without the inclusion of these parameters. Performance measures after calibration showed consistency with actual field values; however, no standard criteria for calibration were defined. Paz et al. [3, 6] calibrated microscopic traffic flow models by taking into consideration the entire set of model parameters simultaneously. The simultaneous selection of all parameters was motivated by the need to seek convergence and stability of the solutions. All parameters were treated equally, and a subset of parameters that may significantly affect a traffic model was not identified. Kim [13] used a bilevel framework to calibrate driver-behavior parameters and O-D demand simultaneously. The calibration was performed only on a congested network.

State-of-the-art methods take into consideration sets of links and parameters for calibration without providing flexibility for selecting or constraining the search space in terms of where and what to use to fine-tune the traffic flow simulation model. In practice, only a subset of links and parameters can be used for calibration; for example, certain links of a network may be precalibrated, and/or default or prespecified values are required by local governance. That is, development and calibration may be restricted to adjust only a subset of all the potentially available parameters in a traffic flow model. Based on local knowledge and experience, key parameters and specific traffic facilities are selected or allowed for calibration [13, 24]. While a large number of parameters increase computational complexity, identifying a subset of important parameters mitigates this problem and increases the ability of an algorithm to find a global optimum [25]. When all the parameters are calibrated simultaneously, lesser-known parameters may yield values that are unexplainable or inconsistent with real-world traffic behavior.

Unlike traditional approaches that either involve a sequential process or consider all parameters simultaneously, this research proposes a methodology that enables the simultaneous selection of specific links/facilities and parameters for calibration. That is, any combination of traffic facilities and model parameters within each facility can be selected simultaneously for calibration. Local and global calibration parameters were taken into consideration. The capability of selecting where and what to calibrate was motivated by requirements to use local knowledge and governance in order to select parameters for calibration. This is of practical and theoretical importance, and these analyses and associated insights are missing in the literature. Our experiments illustrate the consequences of selecting only a subset rather than all parameters.

## 2. Methods

The calibration methodology used in this study was adapted from Paz et al. [3]. This modified approach has the capability to select links and model parameters. The calibration problem was formulated using a mathematical

programming approach. The normalized root mean square, which was the objective function for this study, measured the relative difference between actual and simulated traffic volumes and speeds. Normalization allowed multiple performance measures to be considered simultaneously [3].

## 2.1. Problem Formulation

**2.1.1. Notation and Terms.** In this study, any number and combination of local and global parameters could be selected for calibration. Indicator variables  $\delta_k^p$  and  $\delta^g$  were used to define which parameters were selected. The following are the notations and terms used in this study:

$K$ : set of links selected for calibration

$k$ : subscript for a link selected for calibration,  $k \in K$

$P$ : set of local model parameters

$p$ : superscript for a local model parameter,  $p \in P$

$\alpha_k^p$ : local parameter  $p$  on link  $k$  selected for calibration,  $\forall k \in K$  and  $p \in P$

$\alpha_k$ : set of local parameters on link  $k$  selected for calibration,  $\forall k \in K$

$\delta_k^p$ : indicator variable for local parameter  $p$  on link  $k$  selected for calibration,  $\forall k \in K$ ,  $p \in P$ , and  $\delta_k^p = 1 \Leftrightarrow \alpha_k^p \in \alpha_k$ ; otherwise,  $\delta_k^p = 0$

$\alpha$ : set of local parameters selected for calibration,  $\alpha \in P$

$G$ : set of global model parameters

$g$ : superscript for a global model parameter,  $g \in G$

$\beta^g$ : global parameter selected for calibration  $g$ ,  $\forall g \in G$

$\beta$ : set of global parameters selected for calibration,  $\beta \in G$

$\delta^g$ : indicator variable for global parameter  $g$  selected for calibration,  $\forall g \in G$  and  $\delta^g = 1 \Leftrightarrow \beta^g \in \beta$ ; otherwise,  $\delta^g = 0$

$\theta$ : set of all parameters selected for calibration,  $\theta = \alpha \cup \beta$

$L$ : set of links with actual field data

$l$ : subscript for a link with actual field data,  $l \in L$

$T$ : total number of time periods

$t$ : subscript for a time period,  $t \in T$

$V_{l,t}$ : actual volume for link  $l$  at time period  $t$ ,  $\forall t \in T$  and  $l \in L$

$S_{l,t}$ : actual speed for link  $l$  at time period  $t$ ,  $\forall t \in T$  and  $l \in L$

$W_v$ : weight factor for volumes

$\widehat{V}(\theta)_{l,t}$ : simulated volume for link  $l$  at time period  $t$ ,  $\forall t \in T$  and  $l \in L$

$\widehat{S}(\theta)_{l,t}$ : simulated speed for link  $l$  at time period  $t$ ,  $\forall t \in T$  and  $l \in L$

**2.1.2. Mathematical Program.** The objective function and the calibration criteria were evaluated using links  $L$  with the actual field data that were available.

**(1) Objective Function.** The objective was to minimize the normalized weighted root-mean-square (NRMS) error over the number of time periods ( $T$ ) and links ( $L$ ) as follows:

$$\begin{aligned} \text{minimize NRMS} &= \frac{1}{\sqrt{|L|} + \sqrt{|T|}} \\ &* \sum_{t=1}^T \sum_{l=1}^L \left( W_v * \sqrt{\sum_l^{|L|} \left( \frac{V_{l,t} - \widehat{V}(\theta)_{l,t}}{V_{l,t}} \right)^2} \right. \\ &\left. + (1 - W_v) * \sqrt{\sum_l^{|L|} \left( \frac{S_{l,t} - \widehat{S}(\theta)_{l,t}}{S_{l,t}} \right)^2} \right), \end{aligned} \quad (1)$$

subject to

$$\alpha_k = \{ \alpha_k^p \mid \forall \delta_k^p = 1, \forall k \in K, p \in P \}, \quad (2)$$

$$\alpha = \bigcup_{k \in K} \alpha_k, \quad (3)$$

$$\beta = \{ \beta^g \mid \forall \delta^g = 1, \forall g \in G \}, \quad (4)$$

$$\theta = \alpha \cup \beta, \quad (5)$$

$$\text{lower bound} \leq \alpha_k^p \leq \text{upper bound}, \quad \forall k \in K, p \in P, \quad (6)$$

$$\text{lower bound} \leq \beta^g \leq \text{upper bound}, \quad \forall g \in G. \quad (7)$$

This NRMS error function measures the relative difference between the estimated and the actual volume and speed values. The values in the squared root are the relative differences in volume and speeds for all links selected for calibration that contained actual field data. The relative differences are multiplied by  $W_v$  and  $1 - W_v$  to consider the reliability of volume and speed data. This difference is also measured for all considered time periods. The total error is normalized by dividing it by the squared root of the number of links and time periods considered for calibration. The NRMS is based on a previous study [3], where this error function was used successfully to calibrate traffic flow models.

Constraints (2) and (3) ensured that the local parameters selected for calibration were included in vector  $\theta$ . Similarly, constraint (4) ensured that the global parameters selected for calibration were included in vector  $\theta$ . Constraint (5) was a definitional constraint for the calibration vector  $\theta$ . Constraints (6) and (7) provided the lower and upper bounds for each parameter selected for calibration.

**2.2. Calibration Criteria.** The criterion for calibration is based on guidelines provided by the FHWA [2]. For individual links, in more than 85% of cases, the difference between actual and simulated counts should be

- (i) Within 100 vehicles/hour for link volumes less than 700 vehicles/hour

- (ii) Within 15% of field flow for link volumes between 700 and 2700 vehicles/hour
- (iii) Within 400 vehicles/hour for link volumes greater than 2700 vehicles/hour

The sum of all simulated link count errors should be within 5% of all actual link counts. The GEH statistic for individual link flows should be less than 5 for more than 85% of cases [1, 2]. The GEH statistic is given by

$$\text{GEH} = \sqrt{\frac{2(V_l - \widehat{V}(\theta)_l)^2}{V_l + \widehat{V}(\theta)_l}}, \quad (8)$$

where  $V_l$  is the actual traffic volume for link  $l$  and  $\widehat{V}(\theta)_l$  is the corresponding simulated traffic volume.

**2.3. Solution Algorithm.** The proposed mathematical program, as expressed in equations (1) through (7), was solved using a GA, which searches solutions by trying to avoid stopping at local optima and seeking to increase the probability of locating a global optimum [4, 5, 8–14, 26, 27]. In the context of the GA, a population is generated at random, initially. An individual (chromosome) in a population is composed by a set of calibration parameter values (genes) that represent a viable solution. Table 1 provides an example of an individual or chromosome used in this study. The parameters to be calibrated are organized into an array where specific positions are associated with certain links. The quality of the resulting solution is evaluated by a fitness or objective function, as in equation (1). GA creates successive generations of individuals, and the best individuals are stored to create a new population. The implemented GA expands the one proposed by Paz et al. [3] to address constraints (2)–(7) to enable section of links and calibration parameters. Figure 1 provides a flowchart of the GA solution algorithm.

Algorithmic steps are as follows:

Step 1—initialization: an initial population of  $\theta_s$  is randomly generated but constrained to lower and upper bounds in order to maintain model realism.

Step 2—parents' selection: the best 60% of  $\theta_s$  from the initial population are saved. Then, sets of  $\theta$  are generated that represent parents in the population and are paired using a 'roulette wheel selection.'

Step 3—crossover: a crossover is performed at 50%. This process combines parent  $\theta_s$  in order to generate new sets of calibration parameters (i.e., offspring).

Step 4—mutation: approximately 30% of the parameters of each offspring are subjected to small perturbations ( $\pm 1\%$ ) in order to research neighboring solutions.

Step 5—population management strategy: the new offspring  $\theta$  replaces the worst  $\theta_s$  when new  $\theta$  provides a better fitness than older  $\theta_s$ .

Step 6—stopping criteria: if the stopping criterion is met, best  $\theta$  is returned, and the algorithm ends.

Otherwise, it returns to Step 2. The stopping criterion is met by reaching convergence or a prespecified maximum number of generations/iterations. Convergence is researched when the calibration criteria listed above are met.

### 3. Experiments and Results

The proposed methodology and solution algorithm were tested using CORSIM models. CORSIM includes driver-behavior and vehicle performance parameters. Table 2 lists various calibration parameters in CORSIM [3]. Two CORSIM models are used in the experiments and are illustrated in Figure 2. Both models included arterial roads with signalized intersections. For signal-controlled intersections, one of the important parameters was the discharge headway of individual vehicles [2, 28]. The Reno network (Figure 2(a)) represents the Pyramid Highway in Reno, Nevada, and consists of 126 arterial links. Calibration field data were available for 45 of these links.

The local parameters included the mean queue discharge headway and the mean value of start-up lost time. The global parameters included lane change, acceptable gap in near-side cross-traffic for vehicles at a sign, additional time for far-side cross-traffic in the acceptable gap for vehicles at a sign, and the driver's familiarity with path distributions. The McTrans model (Figure 2(b)), provided by McTrans™, consisted of 20 arterial links. This is a well-known model of a synthetic network used only for demonstration and analysis purposes. The default parameters in the McTrans model were considered as calibrated conditions, and the outputs from this model were used as field data for the experiments. Model parameters were randomly modified to represent an uncalibrated model. The local parameters included mean queue discharge headway and mean start-up lost time. Global parameters included the driver's familiarity with path distributions and included the percentage of drivers who knew only one turn movement as well as the percentage of drivers who knew two turn movements.

**3.1. Experimental Setup.** The proposed solution algorithm was implemented using Java™, which is capable of handling complex data structures and mathematical functions. As noted by Paz et al. [3], the implementation used a basic layered architecture, with each layer handling a group of related functions. Volume and speed data were used for the calibration. The CORSIM models were run for a simulation time period of 15 min. The first set of experiments incorporated a selection of links in the network, and the second set of experiments incorporated the simultaneous selection of links and parameters.

**3.2. First Set of Experiments: Selection of Links in the Network.** In the first set of experiments, links were selected for calibration randomly. All global and local parameters for the selected links were considered simultaneously for calibration.

TABLE 1: Example of an individual (chromosome) for calibration of traffic flow models.

Parameter	Mean queue discharge headway (sec)			Mean start-up lost time (sec)			Through traffic (vehicles)			Left-turning traffic (vehicles)		
Values	2.1	2.1	2.4	3.8	4.2	3.6	636	836	912	837	875	642
Link	1	2	3	1	2	3	1	2	3	1	2	3

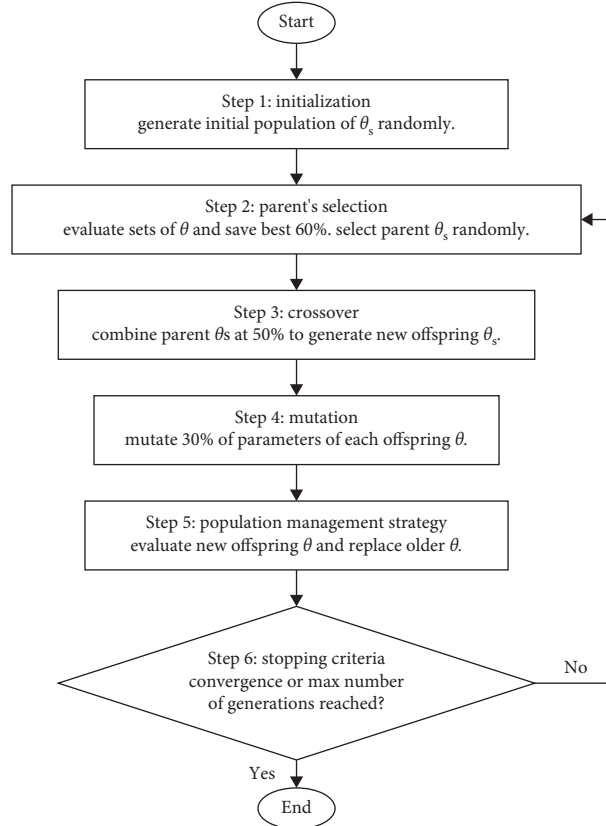


FIGURE 1: Flowchart illustrating the proposed solution algorithm.

When 70% of links were randomly selected, both models were calibrated successfully. Figure 3 shows how the objective function converged when 70% of the links were selected for calibration. The normalized root mean square (NRMS) showed improvement over the iterations of the calibration process. For the Reno network, the initial value of NRMS was 0.22; after 845 iterations, the NRMS decreased to 0.08. For the McTrans model, the initial value of NRMS was 0.29; after 370 iterations, the NRMS decreased to 0.06.

Figure 4 compares vehicle counts before and after calibration. Before calibration, there was a significant difference between the actual and the simulated counts. After calibration, the gap between the actual and simulated counts was reduced, as illustrated by their alignment along the 45° line in Figure 4.

Figure 5 shows the vehicle speeds before and after calibration. For the Reno network, the speed data are scattered away from the 45° line more than the volume data. This is a consequence of a higher weight assigned in the objective

function to volume than speed. Volume data correspond to vehicle counts, while speed is a spot mean measure which is not representative of the actual speed for the entire link.

Figure 6 shows the GEH statistic for the models before and after calibration. For the Reno network, the initial GEH value was less than 5 for 46% of the selected links. After calibration, the GEH value was less than 5 for 93% of the selected links. For the McTrans model, the initial GEH value was less than 5 for 55% of the selected links. After calibration, the GEH value was less than 5 for 100% of the links.

Table 3 outlines the percentage of selected links and the corresponding calibration results when all the parameters were selected simultaneously for calibration. Both models were calibrated successfully when at least 60% of the links were selected. For illustration purposes, Appendix provides the calibration parameters used in the first set of experiments including upper and lower bounds as well as values before and after calibration. All calibrated values are within the accepted range.



TABLE 2: Calibration parameter in CORSIM models [3].

Driver behavior	Vehicle performance	Demand patterns
<i>NETSIM model (surface streets)</i>		
Queue discharge headway	Speed and acceleration characteristics	Surface street turn movements
Start-up lost time		
Distribution of free-flow speed by driver type	Fleet distribution and passenger occupancy	
Mean duration of parking maneuvers		
Lane-change parameters		
Maximum left- and right-turning speeds		
Probability of joining spillback		
Probability of left-turn jumpers and lagers		
Gap acceptance at stop signs		
Gap acceptance for left and right turns		
Pedestrian delays		
Driver familiarity with their path		
<i>FRESIM model (freeways)</i>		
Mean start-up delay at ramp meters	Speed and acceleration characteristics	Freeway turn movements
Distribution of free-flow speed by driver type		
Incident rubbernecking factor	Fleet distribution and passenger occupancy	
Car-following sensitivity factor		
Lane change gap acceptance parameters		
Parameters that affect the number of discretionary lane changes	Maximum deceleration values	

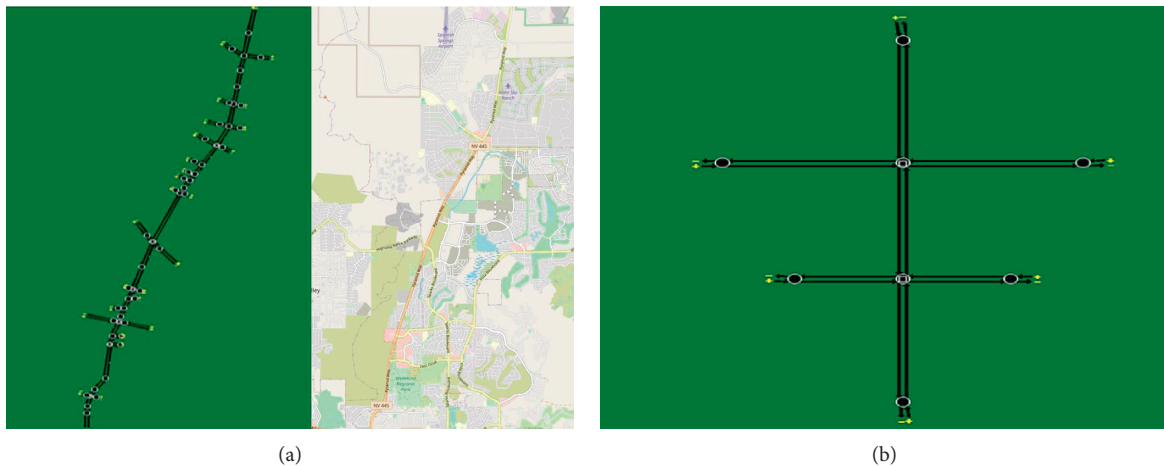


FIGURE 2: CORSIM models used in the experiments: (a) Reno network (Pyramid Highway); (b) McTrans model.

**3.3. Second Set of Experiments: Simultaneous Selection of Links and Parameters.** In the second set of experiments, links and associated parameters were selected simultaneously. These experiments were conducted using different combinations of parameters.

**3.3.1. First Combination.** The local parameters were selected for every link, and the global parameters were set as the default. Table 4 shows the selected percentage of links and the corresponding results when only the local parameters were selected for calibration. The Reno network was calibrated successfully when at least 70% of links were selected for calibration. The McTrans model was successfully calibrated when at least 50% of links were selected for calibration.

**3.3.2. Second Combination.** The mean queue discharge headway was selected as the only local parameter for calibration, and all the global parameters were considered. Table 5 provides the results when the mean queue discharge headway and all the global parameters were selected for calibration. Both models were calibrated successfully when at least 60% of the links were selected for calibration.

**3.3.3. Third Combination.** Mean queue discharge headway and mean start-up lost time were selected as mutually exclusive; meanwhile, all the global parameters were considered for calibration. Table 6 provides the results from using various percentages of the mean queue discharge headway and mean start-up lost time when all global parameters were considered for calibration of the CORSIM models. The Reno

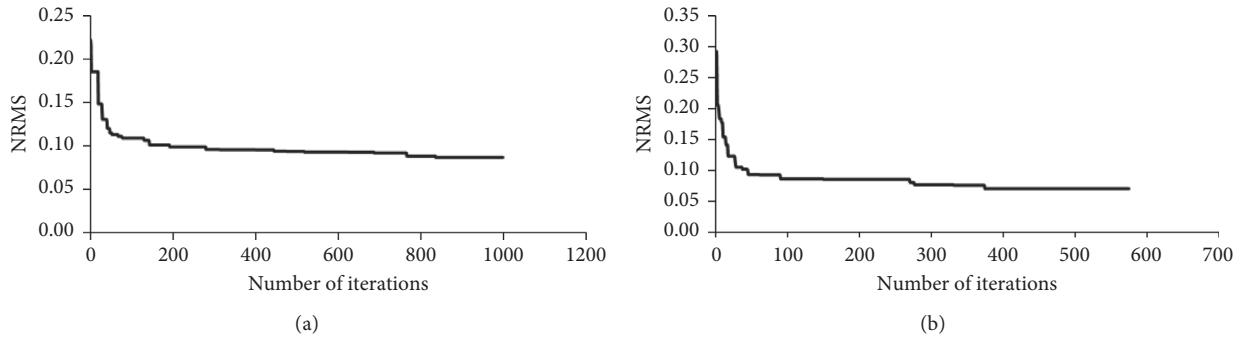


FIGURE 3: Objective function for 70% selection of links for the (a) Reno network and (b) McTrans model.

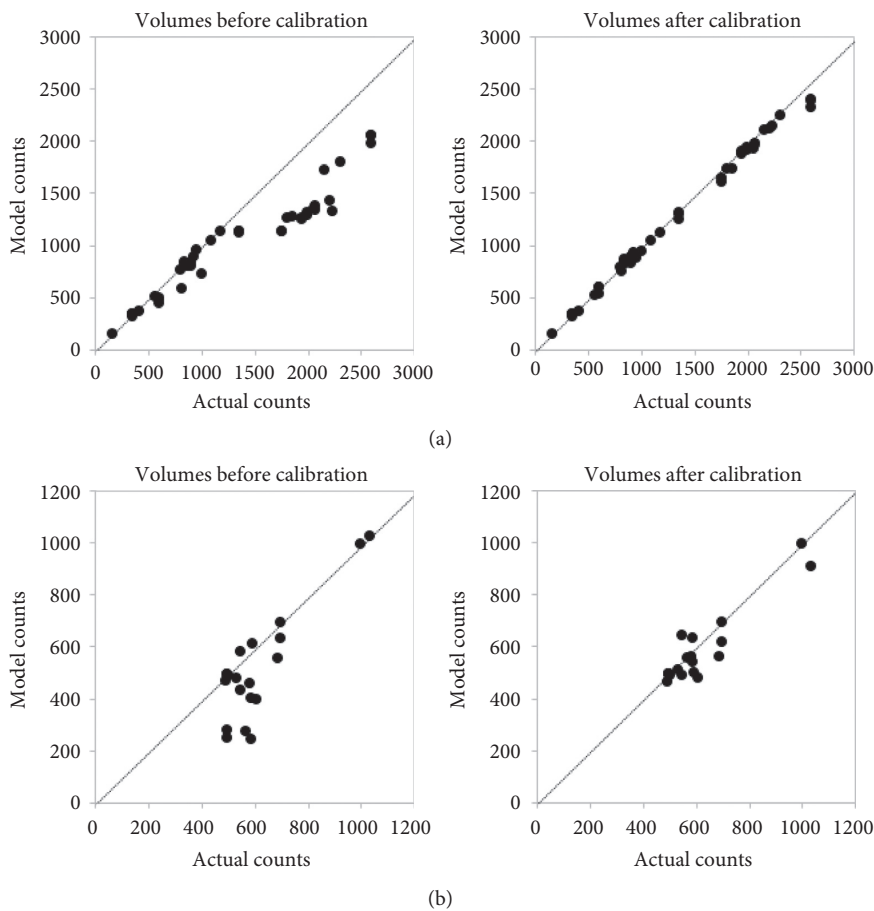
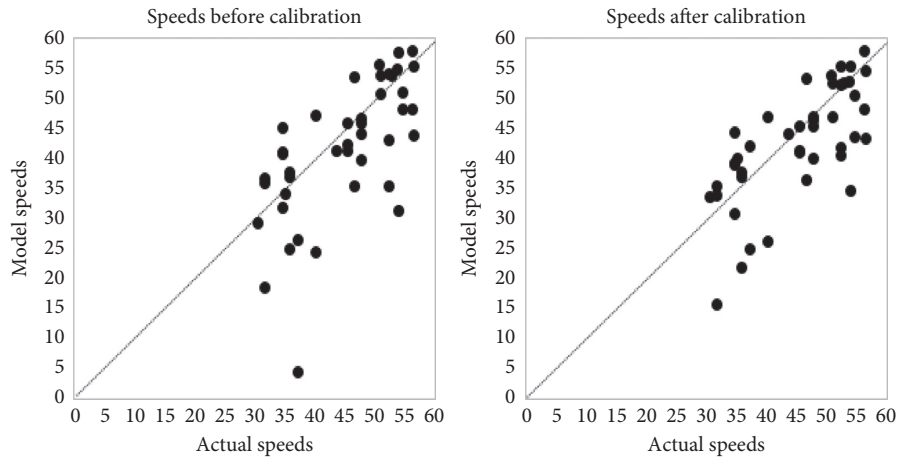


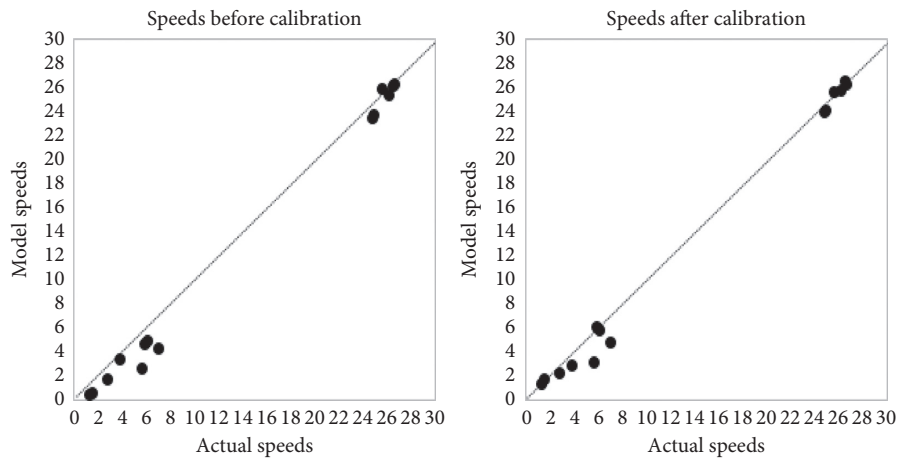
FIGURE 4: Vehicle counts before and after calibration for the (a) Reno model and (b) McTrans model.

network was calibrated successfully when the mean queue discharge headway was selected for at least 80% of links; the mean start-up lost time was selected for the remaining 20% of the links. The McTrans model was calibrated successfully when the mean queue discharge headway was selected for at least 90% of links, and mean start-up lost time was selected for the remaining 10% of links.

3.4. *Sensitivity Analysis.* Sensitivity analyses were conducted to observe the effects on NRMS on various percentage of links and several combinations of parameters selected for calibration. The results are illustrated in Figures 7 and 8. Figure 7 shows the effects on NRMS due to various percentages of links selected for calibration. In Figure 8,

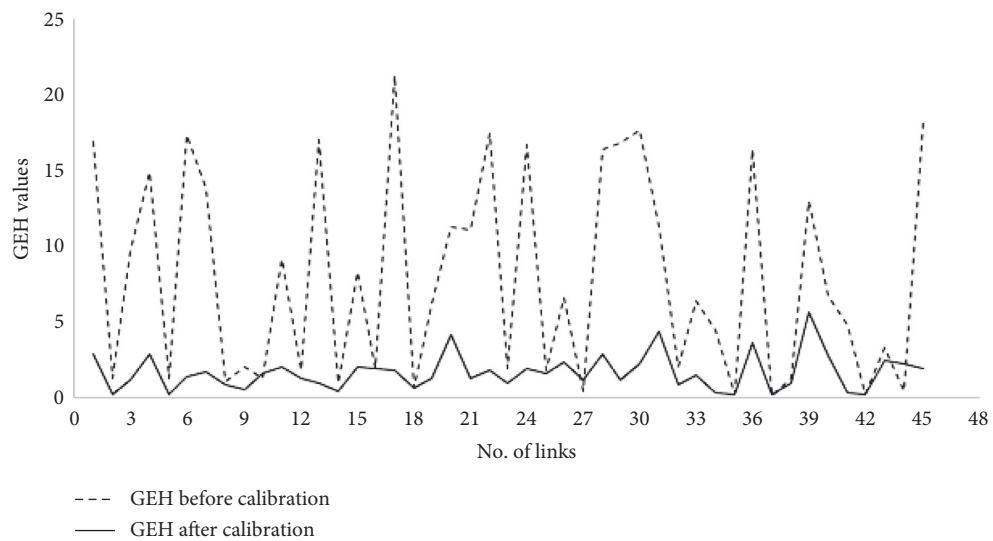


(a)



(b)

FIGURE 5: Speeds before and after calibration for the (a) Reno network and (b) McTrans model.



(a)

FIGURE 6: Continued.



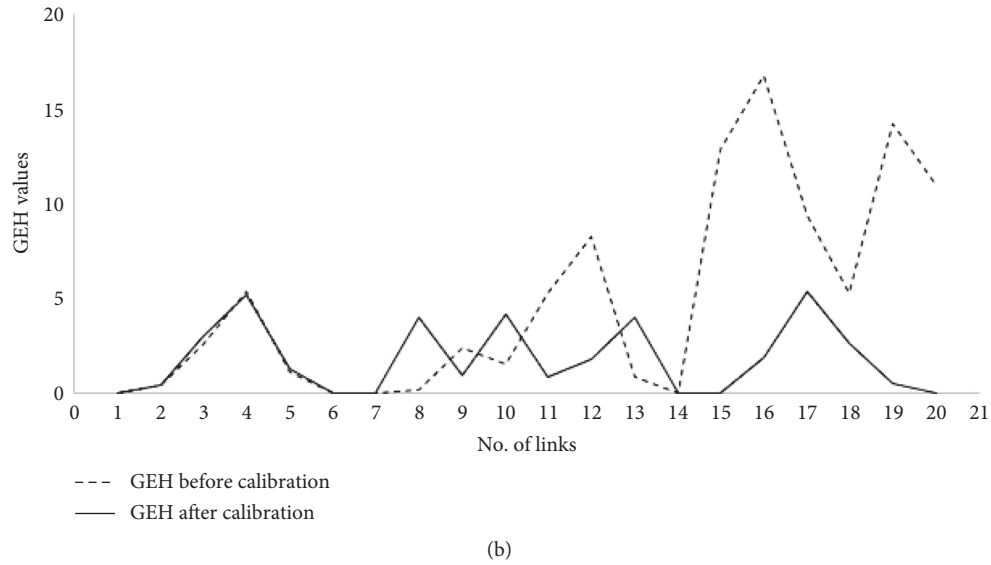


FIGURE 6: GEH statistic before and after calibration for the (a) Reno network and (b) McTrans model.

TABLE 3: Calibration results when all parameters were selected simultaneously.

Percentage of links selected for calibration	NRMS	Individual link flows			Relative difference between total actual and simulated counts	GEH statistic for individual link flows
		<700 veh/hr	700 to 2700 veh/hr	>2700 veh/hr		
For the Reno network						
100	0.0751	100	100	N/A	1.20	<5 for 100%
90	0.0966	100	100	N/A	4.50	<5 for 97%
80	0.0845	100	100	N/A	3.30	<5 for 100%
70	0.0862	100	100	N/A	4.20	<5 for 93%
60	0.0919	100	100	N/A	4.50	<5 for 100%
50	0.1068	88.90	100	N/A	6.90	<5 for 93%
40	0.1119	100	100	N/A	7.30	<5 for 88%
30	0.1285	90	88.60	N/A	10.20	<5 for 73%
20	0.1555	90	57.10	N/A	13.70	<5 for 57%
For the McTrans model						
100	0.0305	100	100	N/A	0.30	<5 for 100%
90	0.0463	100	100	N/A	0.20	<5 for 100%
80	0.0317	100	100	N/A	0.40	<5 for 100%
70	0.0697	100	100	N/A	0.50	<5 for 100%
60	0.1366	89	100	N/A	2.60	<5 for 95%
50	0.1835	72	100	N/A	5.00	<5 for 85%
40	0.1980	78	100	N/A	9.60	<5 for 80%

TABLE 4: Calibration results when only local parameters were selected.

Percentage of links selected for calibration	NRMS	Individual link flows			Relative difference between total actual and simulated counts	GEH statistic for individual link flows
		<700 veh/hr	700 to 2700 veh/hr	>2700 veh/hr		
For the Reno network						
100	0.0884	100	100	N/A	4.00	<5 for 100%
90	0.0860	100	100	N/A	3.20	<5 for 100%
80	0.0873	100	100	N/A	3.10	<5 for 100%
70	0.0946	100	100	N/A	3.40	<5 for 95%
60	0.1369	100	71.4	N/A	11	<5 for 64%
For the McTrans model						
100	0.0480	100	100	N/A	0.60	<5 for 100%

TABLE 4: Continued.

Percentage of links selected for calibration	NRMS	Individual link flows			Relative difference between total actual and simulated counts	GEH statistic for individual link flows
		<700 veh/hr	700 to 2700 veh/hr	>2700 veh/hr		
90	0.0421	100	100	N/A	0.40	<5 for 100%
80	0.1249	89	100	N/A	3.60	<5 for 100%
70	0.0924	94.40	100	N/A	1.40	<5 for 100%
60	0.0974	100	100	N/A	2.70	<5 for 100%
50	0.0959	94.40	100	N/A	3	<5 for 100%
40	0.1367	88.20	66.70	N/A	2.70	<5 for 90%

TABLE 5: Calibration results when all global parameters and mean queue discharge headway were selected.

Percentage of links selected for calibration	NRMS	Individual link flows			Relative difference between total actual and simulated counts	GEH statistic for individual link flows
		<700 veh/hr	700 to 2700 veh/hr	>2700 veh/hr		
For the Reno network						
100	0.0872	100	100	N/A	2.7	<5 for 100%
90	0.0970	100	100	N/A	5.2	<5 for 93%
80	0.0976	100	100	N/A	4	<5 for 97%
70	0.0897	100	100	N/A	3.9	<5 for 100%
60	0.0916	100	100	N/A	5	<5 for 100%
50	0.1037	100	100	N/A	5.9	<5 for 93%
For the McTrans model						
100	0.0860	94.1	100	N/A	1.3	<5 for 95%
90	0.0588	100	100	N/A	0.6	<5 for 100%
80	0.0980	94.4	100	N/A	0.9	<5 for 95%
70	0.1279	88.9	100	N/A	2.2	<5 for 95%
60	0.1257	94.1	100	N/A	2.7	<5 for 95%
50	0.1737	77.8	100	N/A	5.5	<5 for 80%

TABLE 6: Calibration results when selection of the mean queue discharge headway and mean start-up lost time was mutually exclusive.

Percentage of links selected with mean queue discharge headway	Percentage of links selected with mean start-up lost time	NRMS	Individual link flows			Relative difference between total actual and simulated counts (%)	GEH statistic for individual link flows
			<700 veh/hr (%)	700 to 2700 veh/hr (%)	>2700 veh/hr		
For the Reno network							
90	10	0.0909	100	100	N/A	4.2	<5 for 97%
80	20	0.0930	100	100	N/A	4.7	<5 for 100%
70	30	0.0947	100	100	N/A	5.4	<5 for 97%
For the McTrans network							
90	10	0.0679	94.1	100.00	N/A	0.7	<5 for 100%
80	20	0.1827	72.2	100.00	N/A	8.2	<5 for 80%
70	30	0.1746	82.4	66.7	N/A	6.2	<5 for 80%

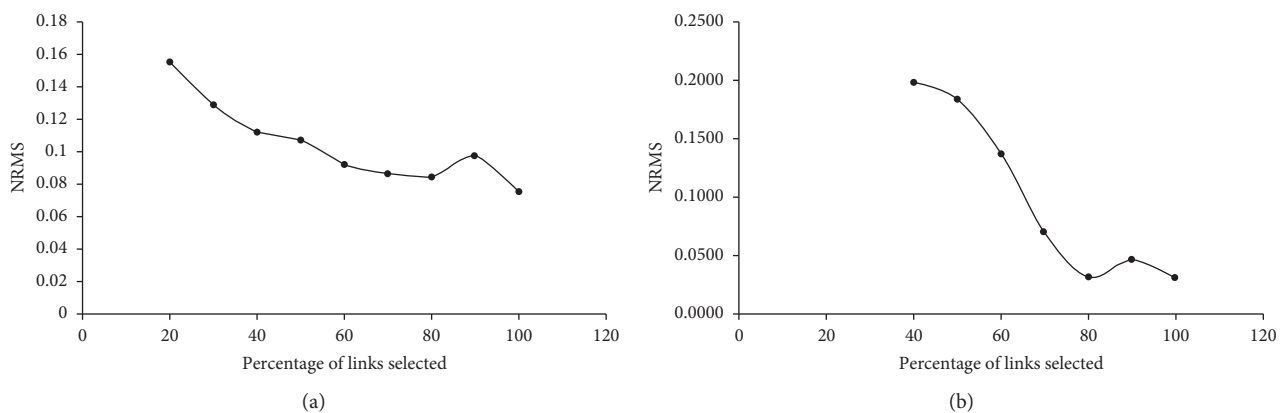


FIGURE 7: Effect on NRMS of various percentages of link selection for calibration. (a) Reno network. (b) McTrans network.

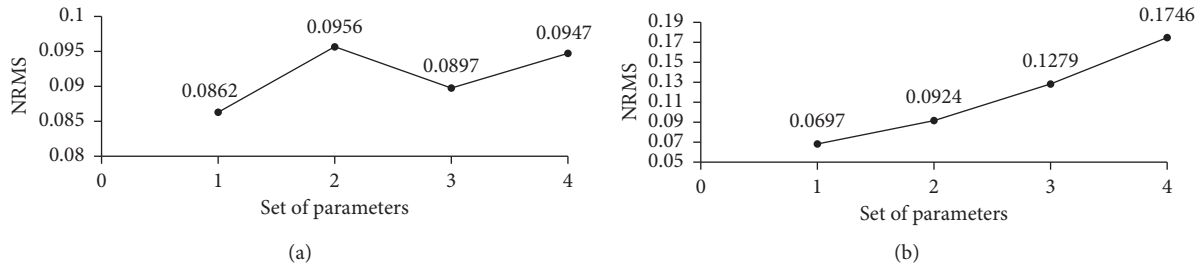


FIGURE 8: Effect on NRMS of various sets of parameters for calibration. (a) Reno network. (b) McTrans network.

TABLE 7: Calibration parameters in the first experiment using the Reno network.

SN	Model	Parameter	Lower bound	Upper bound	Units	Links	Value before calibration	Value after calibration
1	NETSIM	Mean queue discharge headway	14	99	Tenths of seconds	1-26	38	41
2	NETSIM	Mean queue discharge headway	14	99	Tenths of seconds	1-41	36	42
3	NETSIM	Mean queue discharge headway	14	99	Tenths of seconds	2-38	40	42
4	NETSIM	Mean queue discharge headway	14	99	Tenths of seconds	3-27	38	38
5	NETSIM	Mean queue discharge headway	14	99	Tenths of seconds	4-33	36	48
6	NETSIM	Mean queue discharge headway	14	99	Tenths of seconds	4-35	38	85
7	NETSIM	Mean queue discharge headway	14	99	Tenths of seconds	5-42	38	30
8	NETSIM	Mean queue discharge headway	14	99	Tenths of seconds	6-48	38	75
9	NETSIM	Mean queue discharge headway	14	99	Tenths of seconds	7-19	38	48
10	NETSIM	Mean queue discharge headway	14	99	Tenths of seconds	8-21	40	81
11	NETSIM	Mean queue discharge headway	14	99	Tenths of seconds	9-25	36	38
12	NETSIM	Mean queue discharge headway	14	99	Tenths of seconds	10-31	40	56
13	NETSIM	Mean queue discharge headway	14	99	Tenths of seconds	13-39	36	89
14	NETSIM	Mean queue discharge headway	14	99	Tenths of seconds	13-40	38	34
15	NETSIM	Mean queue discharge headway	14	99	Tenths of seconds	14-43	36	40
16	NETSIM	Mean queue discharge headway	14	99	Tenths of seconds	14-44	40	42
17	NETSIM	Mean queue discharge headway	14	99	Tenths of seconds	15-47	40	48
18	NETSIM	Mean queue discharge headway	14	99	Tenths of seconds	16-49	26	48
19	NETSIM	Mean queue discharge headway	14	99	Tenths of seconds	16-51	28	61
20	NETSIM	Mean queue discharge headway	14	99	Tenths of seconds	22-45	28	26
21	NETSIM	Mean queue discharge headway	14	99	Tenths of seconds	11-10	28	48
22	NETSIM	Mean queue discharge headway	14	99	Tenths of seconds	2-3	26	36
23	NETSIM	Mean queue discharge headway	14	99	Tenths of seconds	11-12	30	44
24	NETSIM	Mean queue discharge headway	14	99	Tenths of seconds	12-11	30	32
25	NETSIM	Mean queue discharge headway	14	99	Tenths of seconds	5-6	26	50
26	NETSIM	Mean queue discharge headway	14	99	Tenths of seconds	12-13	23	21
27	NETSIM	Mean queue discharge headway	14	99	Tenths of seconds	13-12	30	22
28	NETSIM	Mean queue discharge headway	14	99	Tenths of seconds	6-5	30	30
29	NETSIM	Mean queue discharge headway	14	99	Tenths of seconds	13-14	30	38
30	NETSIM	Mean queue discharge headway	14	99	Tenths of seconds	14-15	48	90
31	NETSIM	Mean queue discharge headway	14	99	Tenths of seconds	15-14	48	18
32	NETSIM	Mean queue discharge headway	14	99	Tenths of seconds	3-4	45	15
33	NETSIM	Mean queue discharge headway	14	99	Tenths of seconds	51-16	38	28
34	NETSIM	Mean queue discharge headway	14	99	Tenths of seconds	17-1	34	38
35	NETSIM	Mean queue discharge headway	14	99	Tenths of seconds	20-2	34	38
36	NETSIM	Mean queue discharge headway	14	99	Tenths of seconds	43-14	30	34
37	NETSIM	Mean queue discharge headway	14	99	Tenths of seconds	21-8	38	28
38	NETSIM	Mean queue discharge headway	14	99	Tenths of seconds	22-1	34	24
39	NETSIM	Mean queue discharge headway	14	99	Tenths of seconds	23-8	34	19
40	NETSIM	Mean queue discharge headway	14	99	Tenths of seconds	44-14	38	90
41	NETSIM	Mean queue discharge headway	14	99	Tenths of seconds	24-9	30	34
42	NETSIM	Mean queue discharge headway	14	99	Tenths of seconds	52-5	38	38
43	NETSIM	Mean queue discharge headway	14	99	Tenths of seconds	26-1	30	57
44	NETSIM	Mean queue discharge headway	14	99	Tenths of seconds	30-9	30	67
45	NETSIM	Mean queue discharge headway	14	99	Tenths of seconds	30-10	28	70

TABLE 7: Continued.

SN	Model	Parameter	Lower bound	Upper bound	Units	Links	Value before calibration	Value after calibration
46	NETSIM	Mean queue discharge headway	14	99	Tenths of seconds	33-4	26	20
47	NETSIM	Mean queue discharge headway	14	99	Tenths of seconds	28-15	30	74
48	NETSIM	Mean queue discharge headway	14	99	Tenths of seconds	35-4	30	26
49	NETSIM	Mean queue discharge headway	14	99	Tenths of seconds	54-16	28	30
50	NETSIM	Mean queue discharge headway	14	99	Tenths of seconds	49-16	28	32
51	NETSIM	Mean queue discharge headway	14	99	Tenths of seconds	55-7	26	26
52	NETSIM	Mean queue discharge headway	14	99	Tenths of seconds	40-13	20	14
53	NETSIM	Mean queue discharge headway	14	99	Tenths of seconds	41-1	28	14
54	NETSIM	Mean queue discharge headway	14	99	Tenths of seconds	55-8	30	22
55	NETSIM	Mean queue discharge headway	14	99	Tenths of seconds	27-3	36	38
56	NETSIM	Mean queue discharge headway	14	99	Tenths of seconds	4-52	36	38
57	NETSIM	Mean queue discharge headway	14	99	Tenths of seconds	31-10	38	74
58	NETSIM	Mean queue discharge headway	14	99	Tenths of seconds	17-20	38	32
59	NETSIM	Mean queue discharge headway	14	99	Tenths of seconds	2-20	36	96
60	NETSIM	Mean queue discharge headway	14	99	Tenths of seconds	34-11	38	89
61	NETSIM	Mean queue discharge headway	14	99	Tenths of seconds	28-54	40	87
62	NETSIM	Mean queue discharge headway	14	99	Tenths of seconds	16-54	36	22
63	NETSIM	Mean queue discharge headway	14	99	Tenths of seconds	7-55	40	48
64	NETSIM	Mean queue discharge headway	14	99	Tenths of seconds	38-2	36	24
65	NETSIM	Mean queue discharge headway	14	99	Tenths of seconds	8-55	36	59
66	NETSIM	Mean queue discharge headway	14	99	Tenths of seconds	25-9	50	50
67	NETSIM	Mean queue discharge headway	14	99	Tenths of seconds	8018-18	40	42
68	NETSIM	Mean queue discharge headway	14	99	Tenths of seconds	8021-21	50	46
69	NETSIM	Mean queue discharge headway	14	99	Tenths of seconds	8023-23	44	40
70	NETSIM	Mean queue discharge headway	14	99	Tenths of seconds	8024-24	48	50
71	NETSIM	Mean queue discharge headway	14	99	Tenths of seconds	8027-27	46	36
72	NETSIM	Mean queue discharge headway	14	99	Tenths of seconds	8031-31	48	45
73	NETSIM	Mean queue discharge headway	14	99	Tenths of seconds	8033-33	44	50
74	NETSIM	Mean queue discharge headway	14	99	Tenths of seconds	8035-35	50	87
75	NETSIM	Mean queue discharge headway	14	99	Tenths of seconds	8038-38	48	23
76	NETSIM	Mean queue discharge headway	14	99	Tenths of seconds	8039-39	49	51
77	NETSIM	Mean queue discharge headway	14	99	Tenths of seconds	8040-40	40	92
78	NETSIM	Mean queue discharge headway	14	99	Tenths of seconds	8041-41	50	21
79	NETSIM	Mean queue discharge headway	14	99	Tenths of seconds	8043-43	48	46
80	NETSIM	Mean queue discharge headway	14	99	Tenths of seconds	8045-45	18	14
81	NETSIM	Mean queue discharge headway	14	99	Tenths of seconds	8046-46	26	34
82	NETSIM	Mean queue discharge headway	14	99	Tenths of seconds	8048-48	26	76
83	NETSIM	Mean queue discharge headway	14	99	Tenths of seconds	8050-50	26	93
84	NETSIM	Mean queue discharge headway	14	99	Tenths of seconds	8051-51	40	38
85	NETSIM	Mean queue discharge headway	14	99	Tenths of seconds	20-17	40	24
86	NETSIM	Mean queue discharge headway	14	99	Tenths of seconds	54-28	48	52
87	NETSIM	Mean queue discharge headway	14	99	Tenths of seconds	9-8	48	18
88	NETSIM	Mean queue discharge headway	14	99	Tenths of seconds	8-9	40	32
89	NETSIM	Mean value of start-up lost time	0	99	Tenths of seconds	1-26	40	46
90	NETSIM	Mean value of start-up lost time	0	99	Tenths of seconds	1-41	42	20
91	NETSIM	Mean value of start-up lost time	0	99	Tenths of seconds	2-38	40	26
92	NETSIM	Mean value of start-up lost time	0	99	Tenths of seconds	3-27	42	40
93	NETSIM	Mean value of start-up lost time	0	99	Tenths of seconds	4-33	42	93
94	NETSIM	Mean value of start-up lost time	0	99	Tenths of seconds	4-35	42	40
95	NETSIM	Mean value of start-up lost time	0	99	Tenths of seconds	5-42	42	26
96	NETSIM	Mean value of start-up lost time	0	99	Tenths of seconds	6-48	38	20
97	NETSIM	Mean value of start-up lost time	0	99	Tenths of seconds	7-19	40	52
98	NETSIM	Mean value of start-up lost time	0	99	Tenths of seconds	8-21	40	42
99	NETSIM	Mean value of start-up lost time	0	99	Tenths of seconds	9-25	38	40
100	NETSIM	Mean value of start-up lost time	0	99	Tenths of seconds	10-31	38	37
101	NETSIM	Mean value of start-up lost time	0	99	Tenths of seconds	13-39	42	50
102	NETSIM	Mean value of start-up lost time	0	99	Tenths of seconds	13-40	40	92
103	NETSIM	Mean value of start-up lost time	0	99	Tenths of seconds	14-43	20	81

TABLE 7: Continued.

SN	Model	Parameter	Lower bound	Upper bound	Units	Links	Value before calibration	Value after calibration
104	NETSIM	Mean value of start-up lost time	0	99	Tenths of seconds	14-44	20	60
105	NETSIM	Mean value of start-up lost time	0	99	Tenths of seconds	15-47	21	15
106	NETSIM	Mean value of start-up lost time	0	99	Tenths of seconds	16-49	20	43
107	NETSIM	Mean value of start-up lost time	0	99	Tenths of seconds	16-51	20	71
108	NETSIM	Mean value of start-up lost time	0	99	Tenths of seconds	22-45	20	20
109	NETSIM	Mean value of start-up lost time	0	99	Tenths of seconds	11-10	21	34
110	NETSIM	Mean value of start-up lost time	0	99	Tenths of seconds	2-3	21	20
111	NETSIM	Mean value of start-up lost time	0	99	Tenths of seconds	11-12	22	13
112	NETSIM	Mean value of start-up lost time	0	99	Tenths of seconds	12-11	21	72
113	NETSIM	Mean value of start-up lost time	0	99	Tenths of seconds	5-6	28	38
114	NETSIM	Mean value of start-up lost time	0	99	Tenths of seconds	12-13	35	27
115	NETSIM	Mean value of start-up lost time	0	99	Tenths of seconds	13-12	30	39
116	NETSIM	Mean value of start-up lost time	0	99	Tenths of seconds	6-5	30	27
117	NETSIM	Mean value of start-up lost time	0	99	Tenths of seconds	13-14	30	29
118	NETSIM	Mean value of start-up lost time	0	99	Tenths of seconds	14-15	32	33
119	NETSIM	Mean value of start-up lost time	0	99	Tenths of seconds	15-14	28	70
120	NETSIM	Mean value of start-up lost time	0	99	Tenths of seconds	3-4	35	33
121	NETSIM	Mean value of start-up lost time	0	99	Tenths of seconds	51-16	30	63
122	NETSIM	Mean value of start-up lost time	0	99	Tenths of seconds	17-1	42	47
123	NETSIM	Mean value of start-up lost time	0	99	Tenths of seconds	20-2	45	50
124	NETSIM	Mean value of start-up lost time	0	99	Tenths of seconds	43-14	42	44
125	NETSIM	Mean value of start-up lost time	0	99	Tenths of seconds	21-8	40	25
126	NETSIM	Mean value of start-up lost time	0	99	Tenths of seconds	22-1	42	49
127	NETSIM	Mean value of start-up lost time	0	99	Tenths of seconds	23-8	46	36
128	NETSIM	Mean value of start-up lost time	0	99	Tenths of seconds	44-14	40	1
129	NETSIM	Mean value of start-up lost time	0	99	Tenths of seconds	24-9	40	81
130	NETSIM	Mean value of start-up lost time	0	99	Tenths of seconds	52-5	38	2
131	NETSIM	Mean value of start-up lost time	0	99	Tenths of seconds	26-1	40	31
132	NETSIM	Mean value of start-up lost time	0	99	Tenths of seconds	30-9	42	13
133	NETSIM	Mean value of start-up lost time	0	99	Tenths of seconds	30-10	42	76
134	NETSIM	Mean value of start-up lost time	0	99	Tenths of seconds	33-4	46	52
135	NETSIM	Mean value of start-up lost time	0	99	Tenths of seconds	28-15	18	6
136	NETSIM	Mean value of start-up lost time	0	99	Tenths of seconds	35-4	20	16
137	NETSIM	Mean value of start-up lost time	0	99	Tenths of seconds	54-16	20	14
138	NETSIM	Mean value of start-up lost time	0	99	Tenths of seconds	49-16	18	4
139	NETSIM	Mean value of start-up lost time	0	99	Tenths of seconds	55-7	20	23
140	NETSIM	Mean value of start-up lost time	0	99	Tenths of seconds	40-13	25	19
141	NETSIM	Mean value of start-up lost time	0	99	Tenths of seconds	41-1	30	89
142	NETSIM	Mean value of start-up lost time	0	99	Tenths of seconds	55-8	32	24
143	NETSIM	Mean value of start-up lost time	0	99	Tenths of seconds	27-3	32	26
144	NETSIM	Mean value of start-up lost time	0	99	Tenths of seconds	4-52	30	34
145	NETSIM	Mean value of start-up lost time	0	99	Tenths of seconds	31-10	30	47
146	NETSIM	Mean value of start-up lost time	0	99	Tenths of seconds	17-20	30	90
147	NETSIM	Mean value of start-up lost time	0	99	Tenths of seconds	2-20	30	34
148	NETSIM	Mean value of start-up lost time	0	99	Tenths of seconds	34-11	30	34
149	NETSIM	Mean value of start-up lost time	0	99	Tenths of seconds	28-54	40	50
150	NETSIM	Mean value of start-up lost time	0	99	Tenths of seconds	16-54	42	44
151	NETSIM	Mean value of start-up lost time	0	99	Tenths of seconds	7-55	48	29
152	NETSIM	Mean value of start-up lost time	0	99	Tenths of seconds	38-2	42	30
153	NETSIM	Mean value of start-up lost time	0	99	Tenths of seconds	8-55	42	0
154	NETSIM	Mean value of start-up lost time	0	99	Tenths of seconds	25-9	42	44
155	NETSIM	Mean value of start-up lost time	0	99	Tenths of seconds	8018-18	40	38
156	NETSIM	Mean value of start-up lost time	0	99	Tenths of seconds	8021-21	40	42
157	NETSIM	Mean value of start-up lost time	0	99	Tenths of seconds	8023-23	42	99
158	NETSIM	Mean value of start-up lost time	0	99	Tenths of seconds	8024-24	42	38
159	NETSIM	Mean value of start-up lost time	0	99	Tenths of seconds	8027-27	40	40
160	NETSIM	Mean value of start-up lost time	0	99	Tenths of seconds	8031-31	40	70
161	NETSIM	Mean value of start-up lost time	0	99	Tenths of seconds	8033-33	46	40



TABLE 7: Continued.

SN	Model	Parameter	Lower bound	Upper bound	Units	Links	Value before calibration	Value after calibration
162	NETSIM	Mean value of start-up lost time	0	99	Tenths of seconds	8035-35	40	45
163	NETSIM	Mean value of start-up lost time	0	99	Tenths of seconds	8038-38	40	74
164	NETSIM	Mean value of start-up lost time	0	99	Tenths of seconds	8039-39	47	92
165	NETSIM	Mean value of start-up lost time	0	99	Tenths of seconds	8040-40	43	51
166	NETSIM	Mean value of start-up lost time	0	99	Tenths of seconds	8041-41	41	33
167	NETSIM	Mean value of start-up lost time	0	99	Tenths of seconds	8043-43	41	64
168	NETSIM	Mean value of start-up lost time	0	99	Tenths of seconds	8045-45	42	42
169	NETSIM	Mean value of start-up lost time	0	99	Tenths of seconds	8046-46	40	10
170	NETSIM	Mean value of start-up lost time	0	99	Tenths of seconds	8048-48	42	23
171	NETSIM	Mean value of start-up lost time	0	99	Tenths of seconds	8050-50	40	48
172	NETSIM	Mean value of start-up lost time	0	99	Tenths of seconds	8051-51	40	50
173	NETSIM	Mean value of start-up lost time	0	99	Tenths of seconds	20-17	42	61
174	NETSIM	Mean value of start-up lost time	0	99	Tenths of seconds	54-28	38	24
175	NETSIM	Mean value of start-up lost time	0	99	Tenths of seconds	9-8	38	38
176	NETSIM	Mean value of start-up lost time	0	99	Tenths of seconds	8-9	32	28
177	NETSIM	Duration of a lane-change maneuver	1	8	Seconds		2	3
178	NETSIM	Mean time for a driver to react to a sudden deceleration of the lead vehicle	1	30	Tenths of seconds		5	7
179	NETSIM	Minimum deceleration for lane-changing	1	10	Feet per second square		3	3
180	NETSIM	Difference in the maximum and minimum acceptable deceleration for a mandatory lane change	5	15	Feet per second square		7	15
181	NETSIM	Difference in the maximum and minimum acceptable deceleration for a discretionary lane change	5	15	Feet per second square		5	5
182	NETSIM	Deceleration rate of the lead vehicle	10	15	Feet per second square		10	10
183	NETSIM	Deceleration rate of the follower vehicle	10	15	Feet per second square		10	11
184	NETSIM	Driver-type factor used to compute driver aggressiveness	15	50	N/A		20	39
185	NETSIM	Urgency threshold	0	5	Tenths of a second squared per foot		1	3
186	NETSIM	Safety factor x 10	6	10	Tenths of units		6	8
187	NETSIM	Percentage of drivers who cooperate with a lane changer	10	100	Percentage		30	60
188	NETSIM	Headway below which all drivers will attempt to change lanes	1	30	Tenths of seconds		15	3
189	NETSIM	Headway above which no drivers will attempt to change lanes	30	100	Tenths of seconds		40	40
190	NETSIM	Mean longitudinal distance over which drivers decide to perform one lane change	50	2500	Feet		240	387
191	NETSIM	Acceptable gap for driver type 1	15	75	Tenths of seconds		45	42
192	NETSIM	Acceptable gap for driver type 2	15	75	Tenths of seconds		40	67
193	NETSIM	Acceptable gap for driver type 3	15	75	Tenths of seconds		37	39
194	NETSIM	Acceptable gap for driver type 4	15	75	Tenths of seconds		34	32
195	NETSIM	Acceptable gap for driver type 5	15	75	Tenths of seconds		31	17
196	NETSIM	Acceptable gap for driver type 6	15	75	Tenths of seconds		30	31
197	NETSIM	Acceptable gap for driver type 7	15	75	Tenths of seconds		27	25
198	NETSIM	Acceptable gap for driver type 8	15	75	Tenths of seconds		24	42
199	NETSIM	Acceptable gap for driver type 9	15	75	Tenths of seconds		21	19
200	NETSIM	Acceptable gap for driver type 10	15	75	Tenths of seconds		16	16
201	NETSIM	Additional gap time for crossing 1 lane	10	75	Tenths of seconds		10	41
202	NETSIM	Additional gap time for crossing 2 lanes	10	75	Tenths of seconds		19	19
203	NETSIM	Additional gap time for crossing 3 lanes	10	75	Tenths of seconds		23	25
204	NETSIM	Additional gap time for crossing 4 lanes	10	75	Tenths of seconds		28	31
205	NETSIM	Additional gap time for crossing 5 lanes	10	75	Tenths of seconds		31	24



TABLE 7: Continued.

SN	Model	Parameter	Lower bound	Upper bound	Units	Links	Value before calibration	Value after calibration
206	NETSIM	Additional gap time for crossing 6 lanes	10	75	Tenths of seconds		35	69
207	NETSIM	Additional gap time for crossing 7 lanes	10	75	Tenths of seconds		38	52
208	NETSIM	Additional gap time for crossing 8 lanes	10	75	Tenths of seconds		41	61
209	NETSIM	Additional gap time for crossing 9 lanes	10	75	Tenths of seconds		44	46
210	NETSIM	Additional gap time for crossing 10 lanes	10	75	Tenths of seconds		46	47
211	NETSIM	Percentage of drivers that know only one turn movement	0	100	Percentages		5	22
212	NETSIM	Percentage of drivers that know two turn movements	0	100	Percentages		95	78

TABLE 8: Calibration parameters in the first experiment using the McTrans model.

SN	Model	Parameter	Lower bound	Upper bound	Units	Links	Value before calibration	Value after calibration
1	NETSIM	Mean queue discharge headway	14	99	Tenths of seconds	8001-9	58	37
2	NETSIM	Mean queue discharge headway	14	99	Tenths of seconds	1-9	58	68
3	NETSIM	Mean queue discharge headway	14	99	Tenths of seconds	1-4	58	99
4	NETSIM	Mean queue discharge headway	14	99	Tenths of seconds	4-1	58	14
5	NETSIM	Mean queue discharge headway	14	99	Tenths of seconds	3-1	58	73
6	NETSIM	Mean queue discharge headway	14	99	Tenths of seconds	1-2	58	80
7	NETSIM	Mean queue discharge headway	14	99	Tenths of seconds	2-1	58	38
8	NETSIM	Mean queue discharge headway	14	99	Tenths of seconds	7-2	68	45
9	NETSIM	Mean queue discharge headway	14	99	Tenths of seconds	8004-7	68	69
10	NETSIM	Mean queue discharge headway	14	99	Tenths of seconds	6-2	68	26
11	NETSIM	Mean queue discharge headway	14	99	Tenths of seconds	2-6	68	46
12	NETSIM	Mean queue discharge headway	14	99	Tenths of seconds	2-5	68	89
13	NETSIM	Mean queue discharge headway	14	99	Tenths of seconds	5-2	68	14
14	NETSIM	Mean queue discharge headway	14	99	Tenths of seconds	8006-5	68	72
15	NETSIM	Mean value of start-up lost time	0	99	Tenths of seconds	8001-9	40	59
16	NETSIM	Mean value of start-up lost time	0	99	Tenths of seconds	1-9	40	42
17	NETSIM	Mean value of start-up lost time	0	99	Tenths of seconds	1-4	40	86
18	NETSIM	Mean value of start-up lost time	0	99	Tenths of seconds	4-1	40	17
19	NETSIM	Mean value of start-up lost time	0	99	Tenths of seconds	3-1	40	65
20	NETSIM	Mean value of start-up lost time	0	99	Tenths of seconds	1-2	50	43
21	NETSIM	Mean value of start-up lost time	0	99	Tenths of seconds	2-1	50	35
22	NETSIM	Mean value of start-up lost time	0	99	Tenths of seconds	7-2	50	80

TABLE 8: Continued.

SN	Model	Parameter	Lower bound	Upper bound	Units	Links	Value before calibration	Value after calibration
23	NETSIM	Mean value of start-up lost time	0	99	Tenths of seconds	8004-7	50	47
24	NETSIM	Mean value of start-up lost time	0	99	Tenths of seconds	6-2	50	57
25	NETSIM	Mean value of start-up lost time	0	99	Tenths of seconds	2-6	50	89
26	NETSIM	Mean value of start-up lost time	0	99	Tenths of seconds	2-5	50	66
27	NETSIM	Mean value of start-up lost time	0	99	Tenths of seconds	5-2	50	8
28	NETSIM	Mean value of start-up lost time	0	99	Tenths of seconds	8006-5	50	99
29	NETSIM	Percentage of drivers that know only one turn movement	0	100	Percentages		5	79
30	NETSIM	Percentage of drivers that know two turn movements	0	100	Percentages		95	21

- (i) Set 1 includes all global and local parameters that were selected simultaneously for 70% of the links
- (ii) Set 2 includes global parameters set as default and all local parameters selected for 70% of the links
- (iii) Set 3 includes all global parameters and mean queue discharge headway selected for 70% of the links
- (iv) Set 4 includes all global parameters and mutually exclusive mean queue discharge headway and mean start-up lost time selected at 70% and 30% of the links, respectively

As expected, the results show that most of the time, the NRMS decreased with an increased percentage of selected links for calibration. The NRMS value changed for various sets of parameters for the same percentage of links selected for calibration. In both cases, similar values of NRMS between a calibrated and an uncalibrated condition did not suggest that all calibration criteria were met.

#### 4. Conclusion

This study proposed a methodology that enables the selection of any combination of facilities as well as local and global parameters for the calibration of microsimulation traffic flow models. A mathematical program and solution algorithm were proposed to implement the methodology. Results using two network models and various sensitivity analyses showed that the proposed methodology was effective. The models were calibrated successfully for volumes and speeds, subject to the selection of a minimum number of links for calibration. The percentage of links selected for calibration varied from a minimum percentage to 100%. Similarly, various local parameters were selected for the corresponding links. Multiple experiments were performed by varying the selection of global and local calibration parameters. Unselected parameters were assigned default values.

The experiments were tested using CORSIM models. However, the methodology was developed without taking

into consideration the characteristics of a specific traffic flow simulation model. That is, no information regarding the methods used in CORSIM to propagate flow was used. Future work could involve testing the proposed methodology using other traffic flow simulation models. Similarly, the proposed methodology might be able to provide superior results by means of a multiobjective optimization approach in contrast to the single-objective function used in this study [20].

#### Appendix

##### Calibration Parameters

Tables 7 and 8 show the calibration parameters used in the first set of experiments using CORSIM models.

##### Data Availability

The McTrans model is available at <https://mctrans.ce.ufl.edu/mct/index.php/hcs/hcs-downloads/>. The Reno network and corresponding data are proprietary and cannot be provided by the authors. The Nevada Department of Transportation can provide access to the model and data.

##### Disclosure

This manuscript is based on a thesis by Mr. Kul Shrestha as part of his master's degree in Transportation Engineering from the University of Nevada Las Vegas.

##### Conflicts of Interest

The authors declare that they have no conflicts of interest.

##### Acknowledgments

Special thanks are due to Mrs. Julie Longo for her help in editing this manuscript.

## References

- [1] R. Dowling, A. Skabardonis, J. Halkias, G. McHale, and G. Zammit, "Guidelines for calibration of microsimulation models: framework and applications," *Transportation Research Record: Journal of the Transportation Research Board*, vol. 1876, no. 1, pp. 1–9, 2004.
- [2] P. Holm, D. Tomich, J. Sloboden, and C. Lowrance, "Traffic analysis toolbox volume IV: guidelines for applying CORSIM microsimulation modeling software," Report No. FHWA-HOP-07-079, IV (January), 1–349, ITT Industries, White Plains, NY, USA, 2007, <http://trid.trb.org/view.aspx?id=838485>.
- [3] A. Paz, V. Molano, E. Martinez, C. Gaviria, and C. Arteaga, "Calibration of traffic flow models using a memetic algorithm," *Transportation Research Part C: Emerging Technologies*, vol. 55, no. 4, pp. 432–443, 2015.
- [4] J. Ma, H. Dong, and H. M. Zhang, "Calibration of microsimulation with heuristic optimization methods," *Transportation Research Record: Journal of the Transportation Research Board*, vol. 1999, no. 1, pp. 208–217, 2007.
- [5] M. Jha, G. Gopalan, A. Garms, B. Mahanti, T. Toledo, and M. Ben-Akiva, "Development and calibration of a large-scale microscopic traffic simulation model," *Transportation Research Record: Journal of the Transportation Research Board*, vol. 1876, no. 1, pp. 121–131, 2004.
- [6] A. Paz, V. Molano, and M. Sanchez, "Holistic calibration of microscopic traffic flow models: methodology and real world application studies," *Engineering and Applied Sciences Optimization: Dedicated to the memory of Professor M.G. Karlaftis*, Springer International Publishing, vol. 38, no. 1, New York, NY, USA, 2015.
- [7] K. O. Kim and L. R. Rilett, "Simplex-Based calibration of traffic microsimulation models with intelligent transportation systems data," *Transportation Research Record: Journal of the Transportation Research Board*, vol. 1855, no. 1, pp. 80–89, 2003.
- [8] R.-L. Cheu, X. Jin, K.-C. Ng, Y.-L. Ng, and D. Srinivasan, "Calibration of FRESIM for Singapore expressway using genetic algorithm," *Journal of Transportation Engineering*, vol. 124, no. 6, pp. 526–535, 1998.
- [9] A. L. Cunha, J. E. Bessa Jr., and J. R. Setti, "Genetic algorithm for the calibration of vehicle performance models of microscopic traffic simulators," in *Proceedings of the Portuguese Conference on Artificial Intelligence*, pp. 3–14, Aveiro, Portugal, October 2009.
- [10] K.-O. Kim and L. R. Rilett, "Genetic-algorithm based approach for calibrating microscopic Simulation models," in *Proceedings of the Intelligent Transportation Systems 2001*, pp. 698–704, Turin, Italy, February 2001.
- [11] T. Ma and B. Abdulhai, "Genetic algorithm-based optimization approach and generic tool for calibrating traffic microscopic simulation parameters," *Transportation Research Record: Journal of the Transportation Research Board*, vol. 1800, no. 1, pp. 6–15, 2002.
- [12] B. Park, J. Won, and I. Yun, "Application of microscopic simulation model calibration and validation procedure: case study of coordinated actuated signal system," *Transportation Research Record: Journal of the Transportation Research Board*, vol. 1978, no. 1, pp. 113–122, 2006.
- [13] S. J. Kim, *Simultaneous calibration of a Microscopic Traffic Simulation Model and OD matrix*, Texas A&M University, College Station, TX, USA, PhD Diss., 2006.
- [14] S. Chiappone, O. Giuffrè, A. Granà, R. Mauro, and A. Sferlazza, "Traffic simulation models calibration using speed-density relationship: an automated procedure based on genetic algorithm," *Expert Systems with Applications*, vol. 44, pp. 147–155, 2016.
- [15] Y. Yang, H. Dong, Y. Qin, and Q. Zhang, "Parameter calibration method of microscopic traffic flow simulation models based on orthogonal genetic algorithm," in *Proceedings of the 22nd International Conference on Distributed Multimedia Systems*, Colchester, UK, November 2016.
- [16] R. Balakrishna, C. Antoniou, M. Ben-Akiva, and H. Koutsopoulos, "Calibration of microscopic traffic simulation models: methods and application," *Transportation Research Board: Journal of the Transportation Research Board*, vol. 1999, no. 1, pp. 198–207, 2007.
- [17] J. B. Lee, *Calibration of Traffic Simulation Models Using Simultaneous Perturbation Stochastic Approximation (SPSA) Method Extended through Bayesian Sampling Methodology*, Rutgers The State University of New Jersey-New Brunswick, New Brunswick, NJ, USA, 2008.
- [18] A. Paz, V. Molano, and C. Gaviria, "Calibration of CORSIM models considering all model parameters simultaneously," in *Proceedings of the Intelligent Transportation Systems (ITSC), 2012 15th International IEEE Conference*, pp. 1417–1422, Anchorage, AK, USA, September 2012.
- [19] A. Paz, V. Molano, and A. Khan, "Calibration of microscopic traffic flow models considering all parameters simultaneously," in *Proceedings of the 93rd Annual Meeting of the Transportation Research Board*, Washington, DC, USA, January 2014.
- [20] C. Cobos, C. Daza, C. Martínez et al., "Calibration of microscopic traffic flow simulation models using a memetic algorithm with Solis and Wets local search chaining (MA-SW-Chains)," in *Proceedings of the Ibero-American Conference on Artificial Intelligence*, pp. 365–375, San José, Costa Rica, November 2016.
- [21] C. Cobos, C. Erazo, J. Luna et al., "Multi-objective memetic algorithm based on NSGA-II and simulated annealing for calibrating CORSIM micro-simulation models of vehicular traffic flow," in *Proceedings of the Conference of the Spanish Association for Artificial Intelligence*, pp. 468–476, Salamanca, Spain, September 2016.
- [22] C. Cobos, A. Paz, J. Luna, C. Erazo, and M. Mendoza, "A multi-objective approach for the calibration of microscopic traffic flow simulation models," *IEEE Access*, vol. 8, pp. 103124–103140, 2020.
- [23] A. Halati, H. Lieu, and S. Walker, "CORSIM—corridor traffic simulation model," in *Proceedings of the Traffic Congestion and Traffic Safety in the 21st Century: Challenges, Innovations, and Opportunities*, New York, NY, USA, June 1997.
- [24] B. Ciuffo, V. Punzo, and V. Torrieri, "Comparison of simulation-based and model-based calibrations of traffic-flow microsimulation models," *Transportation Research Record: Journal of the Transportation Research Board*, vol. 2088, no. 1, pp. 36–44, 2008.
- [25] V. Punzo and B. Ciuffo, "How parameters of microscopic traffic flow models relate to traffic dynamics in simulation: implications for model calibration," *Transportation Research Record: Journal of Transportation Research Board*, vol. 2124, no. 1, 2009.
- [26] M. Gen and R. Cheng, *Genetic Algorithms and Engineering Optimization*, Vol. 7, John Wiley & Sons, Tokyo, Japan, 2000.

- [27] D. E. Goldberg, *Genetic Algorithms in Search, Optimization and Machine Learning*, Addison-Wesley, Boston, MA, USA, 1989.
- [28] W. T. Hung, F. Tian, and H. Y. Tong, "Discharge headway at signalized intersections in Hong Kong," *Journal of Advanced Transportation*, vol. 37, no. 1, pp. 105–117, 2003.